ACS Partner Journal

ENVIRONMENT & HEALTH

pubs.acs.org/EnvHealth

Article

Protein Corona Formation on Cadmium-Bearing Nanoparticles: Important Role of Facet-Dependent Binding of Cysteine-Rich Proteins

Yu Qi, Wenyu Guan, Chuanjia Jiang,* Wei Chen, and Tong Zhang*

Cite This: *Environ. Health* 2024, 2, 623–630

Read Online

ACCESS | Metrics & More | Article Recommendations | Supporting Information

ABSTRACT: Cadmium-bearing nanoparticles, such as nanoparticulate cadmium selenide (CdSe) and cadmium sulfide (CdS), widely exist in the environment and originate from both natural and anthropogenic sources. Risk assessment of these nanoparticles cannot be accurate without taking into account the properties of the protein corona that is acquired by the nanoparticles upon biouptake. Here, we show that the compositions of the protein corona on CdSe/CdS nanoparticles are regulated collectively by the surface atomic arrangement of the nanoparticles and the abundance and distribution of cysteine moieties of the proteins in contact with the nanoparticles. A proteomic analysis shows that the observed facet-dependent preferential binding of proteins is mostly related to the cysteine contents of the proteins, among commonly recognized protein properties controlling the formation of the protein corona. Theoretical calculations further demonstrate that the atomic arrangement of surface Cd atoms, as dictated by the exposed facets of the nanoparticles, controls the specific binding mode of the S atoms in the disulfide bonds of the proteins. Supplemental protein adsorption experiments confirm that disulfide bonds remain intact during protein adsorption, making the binding of protein molecules sensitive to the abundance and distribution of Cd-binding moieties and possibly molecular rigidity of the proteins. The significant conformational changes of adsorbed proteins evidenced from a circular dichroism spectroscopy analysis suggest that disrupting the structural stability of proteins may be an additional risk factor of Cd-bearing nanoparticles. These findings underline that the unique properties and behaviors of nanoparticles must be fully considered when evaluating the biological effects and health risks of metal pollutants.

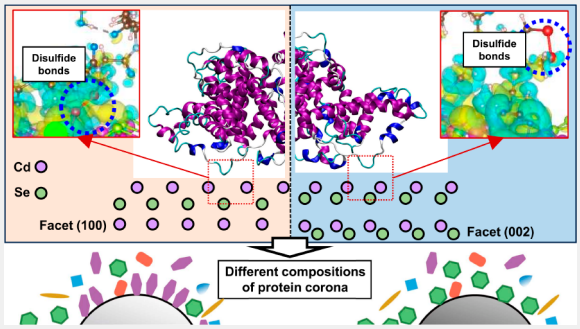

KEYWORDS: *Heavy metal, Mineral nanoparticles, Exposed facet, Protein corona, Preferential adsorption*

1. INTRODUCTION

Cadmium (Cd) is one of the eight metals regulated under the Resource Conservation and Recovery Act (RCRA).[1] In recent years, Cd pollution in the form of Cd-bearing nanoparticles has received increasing attention.[2,3] Cd-containing nanoparticles widely exist in the environment. Natural geological processes, such as mineralization and weathering, generate large quantities of nanosized Cd-containing minerals.[2,4−10] Moreover, Cd-based nanomaterials are projected to be one of the fastest growing groups of engineered nanomaterials in the applications of energy storage, electronic devices, catalysis, medical imaging, and biomedicine.[11−13] The increasing production, application, and disposal of the Cd-based nanomaterials inevitably elevate their environmental release. It is well recognized that the biological effects of heavy metals are strongly dependent on their chemical speciation.[5,6,14] In particular, heavy metals in the nanoparticulate forms interact with bioreceptors in distinctly different manners than their soluble and bulk-sized counterparts.[7−9,12,13] Therefore, holistic and precise assessment of ecological and human-health risks of cadmium pollution calls for the understanding of how the emerging cadmium species (i.e., nanoparticles) react with bioreceptors.

Upon biouptake, nanoparticles rapidly adsorb host proteins in biological fluids and form an organic molecule layer known as the protein corona,[15−20] consisting of proteins exhibiting high binding affinity and slow dissociation rate (i.e., hard corona) and those of low affinity and fast dissociation rate (soft corona).[20] Thus, protein corona formation is the very first step of nanoparticles toward exerting detrimental effects on bioreceptors, as this unique process confers a biological identity to nanoparticles and, consequently, determines the *in vivo* distribution and cellular recognition of the corona−nanoparticle composites.[21−25] The compositions of protein

Received: February 12, 2024
Revised: May 15, 2024
Accepted: May 17, 2024
Published: May 30, 2024

https://doi.org/10.1021/envhealth.4c00031
Environ. Health 2024, 2, 623−630

coronas on nanoparticles are determined by both the physiochemical properties of nanoparticles (e.g., shape, size, exposed facet, surface roughness, functionality, charge, and hydrophobicity) and the properties of proteins (e.g., mass, hydrophobicity, and isoelectric point).[26] Thus far, direct studies on protein corona formation on Cd-bearing nanoparticles are few. Several studies carried out using Cd quantum dots and single proteins identified electrostatic and hydrogen-bonding interactions as the main mechanisms driving protein adsorption.[27,28] In our previous study, we found that the inner-sphere complexation between surface Cd atoms and the protein thiols was a dominating mechanism controlling adsorption of transferrin on cadmoselite and greenockite nanoparticles.[15] Moreover, different facets exhibit different affinities for thiol groups, resulting in facet-dependent preferential binding.[15] Here, we further speculate that exposed facets (as an intrinsic property determining the atomic arrangement and reactivity of surface Cd atoms) and the abundance and distribution of thiol groups of proteins collectively regulate the types and abundance of proteins in the corona.

To test this hypothesis, we chose three pairs of nanosized CdSe and CdS—including two CdSe nanospheres with different contents of the (100) facet, two CdSe nanorods with different contents of the (100) facet, and two CdS nanorods with different contents of the (002) facet—as the model materials, as CdSe and CdS are common Cd-bearing minerals in the environment, and (100) and (002) are the dominant facets of these minerals.[2,11] Each pair of the nanoparticles was synthesized to give similar morphology, size, and electrokinetic properties, so that the effects of exposed facets can be directly compared. The Cd-containing nanoparticles were incubated in matrices containing serum proteins. Proteomic analysis was carried out to understand the preferential binding of the proteins. Theoretical calculations, including molecular dynamics (MD) and ab initio molecular dynamics (AIMD) simulations, were performed to reveal the binding strength and configuration of the proteins. Circular dichroism (CD) spectroscopy analysis was used to examine the conformational changes of proteins upon adsorption. The findings underline the need to consider the unique process of protein corona formation of the nanoparticulate species when assessing the risks of heavy metals.

2. MATERIALS AND METHODS

2.1. Characterization of CdSe and CdS Nanoparticles

Detailed procedures for the preparation of CdSe and CdS nanoparticles are described in the Supporting Information (SI).[15,29] The physical dimensions and morphologies of the Cd-based nanoparticles were characterized by high-resolution transmission electron microscopy (HR-TEM, JEM-2100, JEOL, Japan). The X-ray diffraction (XRD) patterns of the nanoparticles were obtained using a diffractometer (D/MAX2500, Rigaku, Japan) with Cu K radiation (λ = 1.5418 Å). The hydrodynamic diameter (D_h) and ζ-potential of the nanoparticles were determined using a ZetaSizer (Nano ZS, Malvern Instruments, U.K.).

2.2. Formation and Characterization of Corona−Nanoparticle Composites

The CdSe or CdS suspension was sonicated (100 W) for 30 min prior to incubation with 10% (v/v) fetal bovine serum (FBS, Genview, China) at 37 °C. After 4 h, the nanoparticle−protein complexes were separated from the supernatant plasma by centrifugation at 12851*g* (4 °C) for 10 min. The pellet was washed with phosphate-buffered saline (PBS) three times to remove the low-adherence proteins from the nanoparticles (i.e., the soft protein corona). The nanoparticle−protein complexes were resuspended in protein loading buffer (Genview, China), and the suspension was then boiled for 5 min at 100 °C, cooled to room temperature, and centrifuged at 12851*g* (4 °C) for 5 min prior to further analysis.

The composition and structure of the hard protein corona formed on the surface of the nanoparticles were characterized using sodium dodecyl sulfate−polyacrylamide gel electrophoresis (SDS-PAGE) and liquid chromatography−mass spectrometry/mass spectrometry (LC-MS/MS) analysis. Detailed procedures are described in the SI. Afterward, the top 100 proteins according to the order of the Mascot score were selected for protein identity validation.

2.3. Analysis of Weights by Correlation

RapidMiner Studio software (9.4.001, educational edition) was employed to identify the important physiochemical properties of proteins adsorbed on CdSe and CdS nanoparticles, and the auto model was chosen to run the analysis. First, the top 100 proteins from the hard corona on each nanoparticle in one group were combined into one datasheet for further analysis. The relative abundance of proteins in the hard corona (i.e., exponentially modified protein abundance index (emPAI) value) and six biophysicochemical properties of proteins were recorded: molecular weight (Mass), grand average of hydropathicity (GRAVY), theoretical isoelectric point (PI), the numbers of negatively charged residues (NCR, i.e., aspartic acid and glutamic acid) and positively charged residues (PCR, i.e., arginine and lysine), and content of cysteine (Cys%). The entire databases of selectively adsorbed proteins with the six recorded properties were subjected to correlation analysis. Lastly, the weights by correlation were calculated.

2.4. Protein Adsorption Experiments

For adsorption experiments with bovine serum albumin (BSA, Genview, China), the concentrations of CdSe nanospheres and BSA were 200 and 100 μg/mL, respectively. Blank control tests using samples without CdSe nanospheres were also performed, which showed no adsorption of proteins into the vials. After incubation at 37 °C for different times, the complexes were separated by centrifugation at 10709*g* and 4 °C for 10 min, and the supernatant was withdrawn to analyze the concentrations of proteins using the Bradford Protein Assay Kit (Sangon Biotech, China), following the manufacturer's instructions. The adsorbed mass was calculated from protein concentration in solution based on a mass balance approach. Adsorption of BSA on CdSe nanospheres was also simulated using MD and AIMD simulation,[30−35] and detailed procedures are described in the SI.

2.5. Characterization of Conformational Changes of Proteins

To further confirm the interaction between disulfide bonds and CdSe nanospheres, a solution of recombinant human transforming growth factor-β1 (TGF-β1, Peprotech, China, at 50 ng/mL) was incubated with the CdSe nanospheres (100 μg/mL) for 30 min (37 °C), followed by SDS-PAGE. Afterward, the gel was subjected to silver staining using a commercial kit (Solarbio, China). To obtain TGF-β1 monomer, one TGF-β1 sample was mixed with the SDS-PAGE loading buffer (4×, Solarbio, China) containing dithiothreitol (DTT, Solarbio, China) as a positive control. By contrast, the SDS-PAGE loading buffer without DTT was used for experimental groups.

To assess the conformational changes of BSA upon interaction with CdSe nanospheres, the CD spectra of the BSA-CdSe samples were acquired on a J-715 spectropolarimeter (Jasco, Japan) using a quartz cell with a 1 cm path length for the far-UV measurements at room temperature. The concentrations of CdSe nanospheres and proteins were 40 and 20 μg/mL, respectively. Data were collected from 190 to 250 nm by using a response time of 1 s and a scan speed of 100 nm/min. Spectra represented an average of three scans, with the background corrected against deionized (DI) water.

https://doi.org/10.1021/envhealth.4c00031
Environ. Health 2024, 2, 623−630

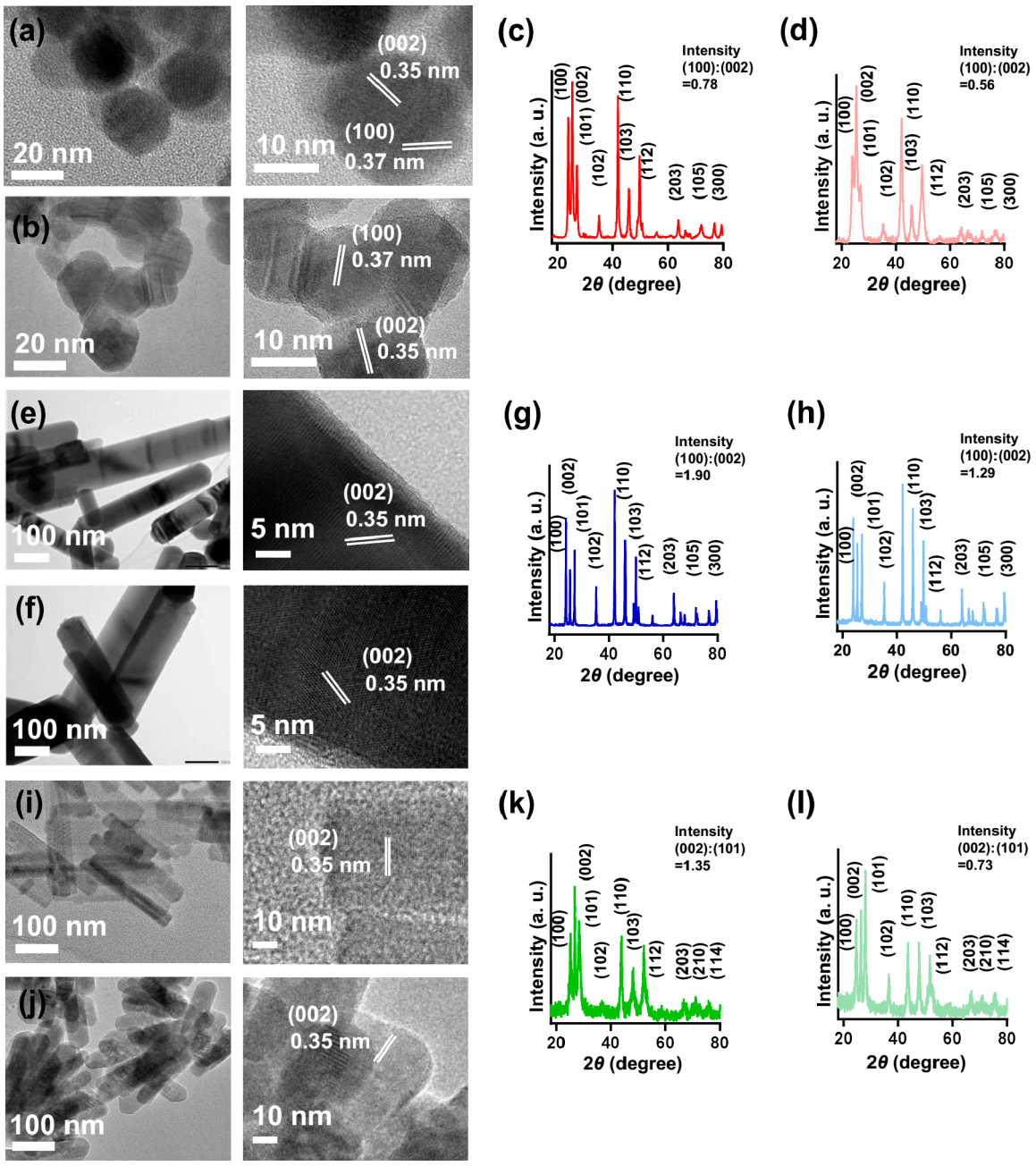

Figure 1. Characterization of differently faceted CdSe and CdS nanoparticles. High-resolution transmission electron microscopy (HR-TEM) images of different-faceted CdSe nanospheres (a, CdSe-s-A; b, CdSe-s-B), CdSe nanorods (c, CdSe-r-A; d, CdSe-r-B), and CdS nanorods (e, CdS-r-A; f, CdS-r-B) and the X-ray diffraction (XRD) patterns of the CdSe nanospheres (g, CdSe-s-A; h, CdSe-s-B), CdSe nanorods (i, CdSe-r-A; j, CdSe-r-B), and CdS nanorods (k, CdS-r-A; l, CdS-r-B). The XRD patterns show that the two nanoparticles in each group had different facet contents (i.e., (100) vs (002) for CdSe and (002) vs (101) for CdS), according to the intensity of the corresponding peaks.

3. RESULTS AND DISCUSSION

3.1. Characterization of Cd-Containing Nanoparticles

The Cd-containing nanoparticles are grouped into three pairs, with each pair exhibiting similar size and morphology but different contents of exposed facets (Figure 1): CdSe nanospheres (i.e., pair 1: coded as CdSe-s-A and CdSe-s-B) with different contents of the (100) facet, CdSe nanorods (pair 2: CdSe-r-A and CdSe-r-B) with different contents of the (100) facet, and CdS nanorods (pair 3: CdS-r-A and CdS-r-B) with different contents of the (002) facet. Based on the TEM images, the CdSe nanospheres had diameters of approximately 20−30 nm (Figure 1a,b), whereas the CdSe and CdS nanorods had dimensions of approximately 400 × 20 nm (Figure 1c,d) and 100 × 10 nm (Figure 1e,f), respectively. The XRD patterns demonstrated that CdSe and CdS were of cadmoselite and greenockite phases, respectively.[15,29] The diffraction peak intensities show the relative contents of different facets. Specifically, the different (100):(002) peak height ratios indicated a higher abundance of the (100) facet in CdSe-s-A and CdSe-r-A than in the corresponding "B" samples, and the different (002):(101) peak height ratios indicated higher (002) facet content of CdS-r-A than in CdS-r-B. The two samples in

https://doi.org/10.1021/envhealth.4c00031
Environ. Health 2024, 2, 623−630

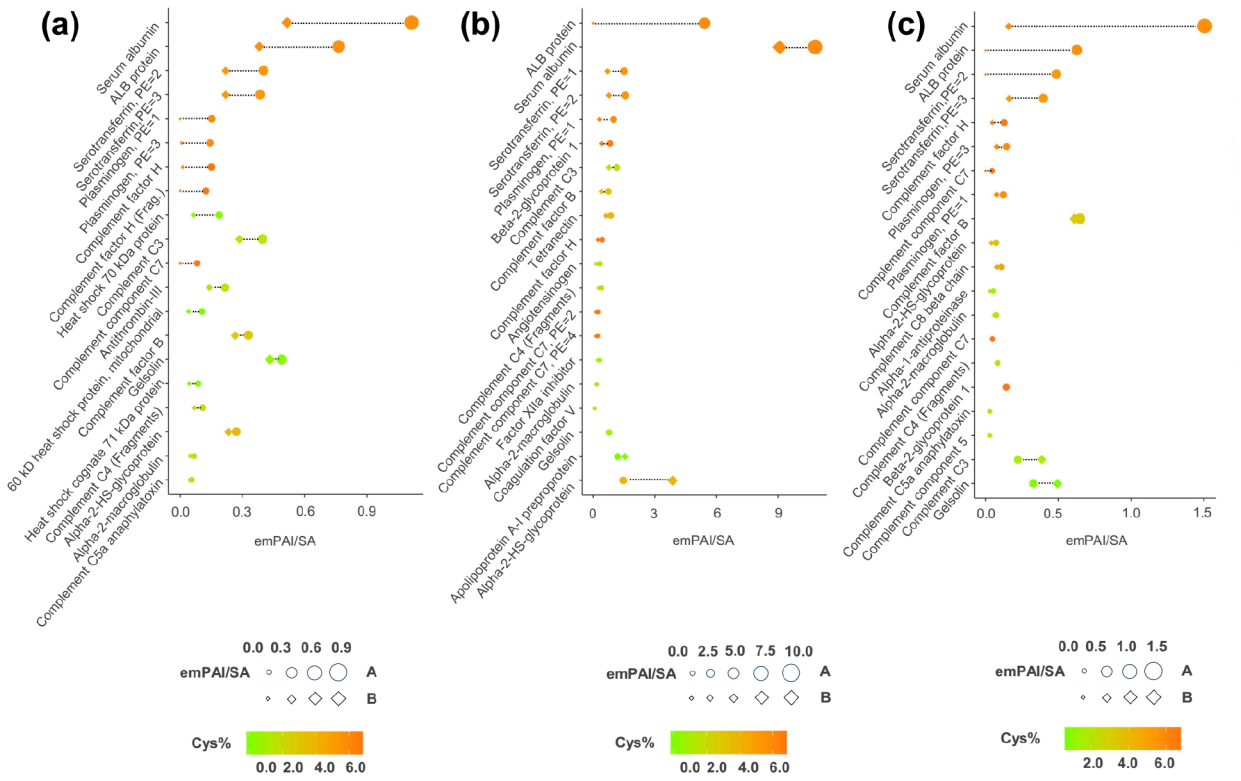

Figure 2. Analysis of the differential protein compositions in the hard corona of the CdSe and CdS nanoparticles. Top 20 most abundant proteins in the hard corona of CdSe or CdS nanoparticles (a, CdSe-s; b, CdSe-r; c, CdS-r), with the size of the circles representing the emPAI/SA values. The proteins were ranked according to the decreasing difference in the absolute emPAI/SA value of proteins determined from the hard coronas on the two CdSe or CdS nanoparticles.

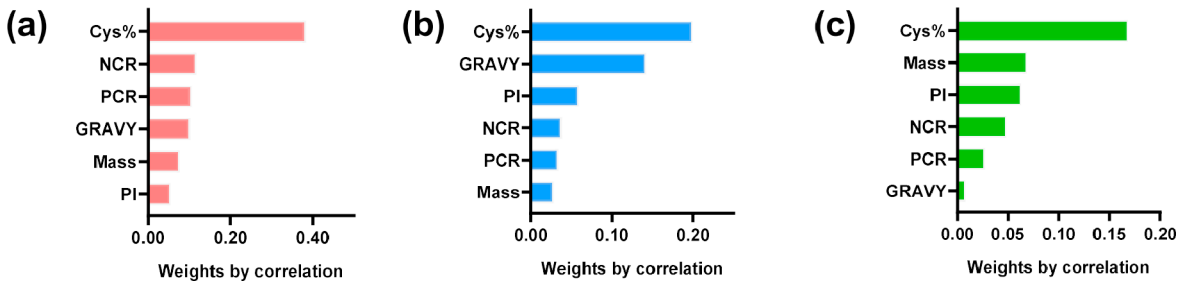

Figure 3. Weights of the biophysicochemical properties of proteins in determining the differential protein adsorption amount (i.e., difference of emPAI/SA value) in the hard corona of CdSe and CdS nanoparticles (a, CdSe-s; b, CdSe-r; c, CdS-r), determined using weight analysis by correlation. Results show that the content of cysteine (Cys%) was the most related property for three groups of nanoparticles.

each group showed similar electrokinetic properties (hydrodynamic diameter and ζ potential, Table S1).

3.2. Exposed Facets of Cd-Bearing Nanoparticles and Cysteine Contents of Proteins Are Determining Factors Controlling Protein Corona Compositions

When the CdSe and CdS nanoparticles were incubated in PBS with 10% FBS, a protein corona formed and a variety of serum proteins were identified from the hard corona, mostly globular proteins, complement components, and transport proteins (Table S1 (SI)). For all three pairs of Cd-bearing nanoparticles, the most abundant proteins in the corona—upon surface area normalization—were serum albumin and ALB protein, and transferrins were the third and fourth most abundant proteins (Figure 2). Within each pair, the two Cd-containing samples acquired similar proteins (i.e., almost all the proteins acquired by material A were also acquired by material B, except the ones of very low abundance; Table S1), but the relative abundance of a given protein—as indicated by the emPAI/SA value (i.e., the emPAI value normalized with the surface area of the nanocrystal)—varied significantly (Figure 2). For example, the emPAI/SA value of serum albumin of CdSe-s-A was 1.11, whereas that of CdSe-s-B was only 0.51. Even larger differences were observed between CdSe-r-A and CdSe-r-B (with a ΔemPAI/SA value of 1.74), and between CdS-r-A and CdS-r-B (ΔemPAI/SA of 1.35). Given the similarities in physicochemical and electrokinetic properties between a given pair of samples, the aforementioned differences in the relative abundance of proteins can be largely attributed to the differences in exposed facets.

An interesting observation was that the proteins of the highest abundance in the corona of the Cd-bearing nanoparticles shared a common trait; that is, these proteins were rich in cysteine content (Figure 2). To quantitatively understand the determining role of cysteine content (Cys%)

https://doi.org/10.1021/envhealth.4c00031
Environ. Health 2024, 2, 623−630

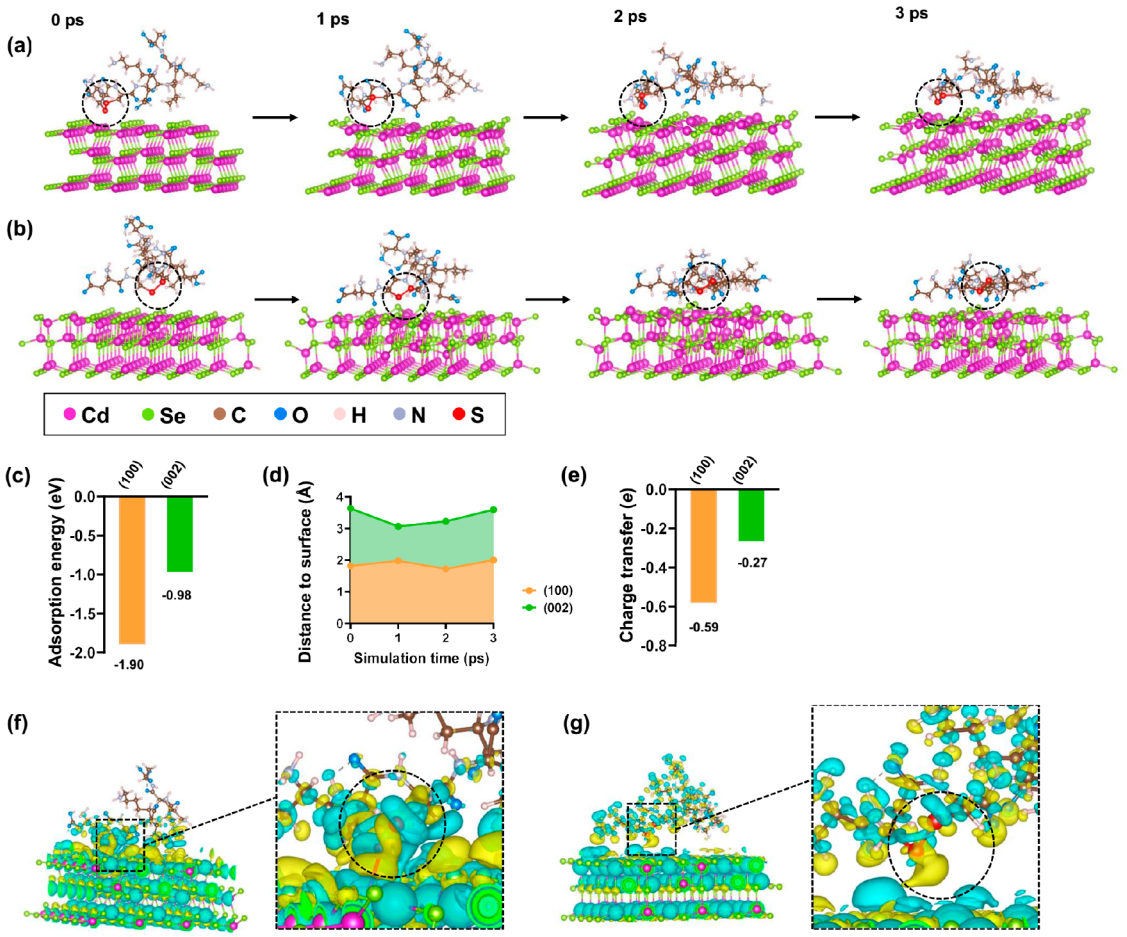

Figure 4. Ab initio molecular dynamics (AIMD) simulation of the specific peptide and CdSe nanoparticles. (a,b) Snapshots of the peptide molecule and CdSe (100) (a) or (002) (b) surface within 3 ps of simulation. The disulfide bond and the bond formed between the S and Cd atoms are marked in black dashed circles. (c) Adsorption energy of the peptide onto the (100) or (002) facet. (d) Relative distance between the S atom and the surface through 3 ps simulation. (e) Bader charge transfer of the peptide onto the (100) or (002) facet. (f,g) Charge density differences of accumulation (i.e., gain of electron density, blue) and depletion (i.e., loss of electron density, yellow) between the peptide and CdSe (100) (f) and (002) (g) surfaces at 3 ps, with the disulfide bond in the peptide marked in black dashed circles.

in protein corona formation, we calculated the correlation factors between ΔemPAI/SA and common protein properties that influence binding of proteins to nanoparticles (Figure S1). Based on the ranking of the correlation factors, Cys% appeared to be the most predominant factor controlling the preferential binding of proteins to all three pairs of CdSe and CdS nanoparticles, much more than other protein properties such as GRAVY (grand average of hydropathy), NCR (negative charge residue), and Mass (Figure 3). These findings underline the critical role of Cd−cysteine interaction in determining the facet-dependent preferential acquisition of proteins.

To further demonstrate that exposed facets of Cd-bearing nanoparticles and cysteine contents of proteins collectively determined corona compositions, we compared the relative abundance of the high-Cys% proteins in the hard corona of the "A" samples vs that in the "B" samples. The proteins examined included serum albumin (Cys% = 5.77), ALB protein (Cys% = 5.77), serotransferrin (Cys% = 6.75), and plasminogen (Cys% = 5.91). Notably, the ΔemPAI/SA values associated with these four proteins were considerably larger than those of the lower-Cys% proteins. For example, the ΔemPAI/SA value of serum albumin of the two CdSe-s samples was 0.60, 7.3 times that of hemoglobin subunit alpha, a protein with a cysteine content of 0. Moreover, supplementary adsorption experiments of BSA, the most abundant protein in the hard corona of all the particles, showed that adsorption of BSA to CdSe-s-A was faster and the adsorbed mass was higher than that to CdSe-s-B (Figure S2). These results were in line with the trend observed in the proteomic analysis; that is, both exposed facets and cysteine content of proteins are determining factors for the specific compositions of corona on Cd-bearing nanoparticles.

3.3. Facets of Nanoparticles and Abundance/Distribution of Disulfide Groups of Proteins Collectively Regulate Binding Configuration of Proteins

Note that even though the calculated correlation factors in Figure 3 showed that the cysteine content was the most important protein property controlling corona formation on Cd-bearing nanoparticles, the contributions of other protein properties cannot be completely neglected. For example, a high correlation of ΔemPAI/SA with GRAVY was observed for the two CdSe-r samples. Similarly, mass and PI (isoelectric point) were secondary protein properties controlling protein binding to the two CdS-r samples. These observations indicated that certain conformational changes of the proteins must have occurred to accommodate the complexation between Cd atoms and sulfur-containing groups of the proteins. Granted, the flexibility of the proteins is to a large extent related to

https://doi.org/10.1021/envhealth.4c00031
Environ. Health 2024, 2, 623−630

protein properties such as molecular weight, hydrophobicity, and charge distribution, as reflected by mass, GRAVY, NCR (negative charge residue) and PI.

To illustrate the molecular level interactions of proteins with different facets of the Cd-containing nanoparticles, we carried out MD and AIMD simulations, using BSA as the model protein and CdSe-s as the model nanoparticles. A BSA molecule was placed above the (100) or (002) facet and allowed to adsorb freely onto the surface through a 20 ns simulation (Figure S3a,b).[17] The MD simulation identified a specific region of the BSA molecule that interacts with both the (100) and (002) facets of CdSe, and this piece of peptide from the BSA molecule (i.e., Ser272-Lys273-Leu274-Lys275-Glu276-Cys277-Cys278-Asp279) (Figure S3c,d), was chosen for the AIMD simulation (Figure 4a,b). Note that in the BSA molecule, the two cysteine residues Cys277 and Cys278 each form a pair of disulfide bonds with another cysteine residue, instead of existing as free thiol groups. Thus, for the AIMD simulation, we manually added a pair of disulfide bonds between Cys277 and Cys278 in the model peptide structure. According to the calculated adsorption energy, it is energetically more favorable for this peptide to bind with the (100) facet than with the (002) facet (Figure 4c). The disulfide bonds tend to make closer contact with the (100) facet than with the (002) facet during the simulation, suggested by the shorter distance between the S atom and the surface over time (Figure 4d). In addition, the change of Bader charge between the peptide and the (100) facet is 0.59 eV, higher than that between the peptide and the (002) facet (0.27 eV) (Figure 4e), which is in line with the higher affinity of the peptide to the (100) facet. Moreover, according to the charge density difference analysis, electron accumulation at the S atom (as indicated by the blue regions in the enlarged portion of Figure 4e) and electron depletion of the Cd atom (the yellow regions) are much more significant on the (100) facet (Figure 4f) than on the (002) facet (Figure 4g), indicating that direct electron transfer between the S atoms of the peptide and the surface Cd atoms is more favorable on the (100) facet.

Notably, even though adsorption of the peptide to the (100) facet is stronger, the binding is not through the complexation of a Cd atom with a thiol group, as the disulfide bonds do not break during protein corona formation (Figure 4a). Rather, the Cd atom appears to interact with one of the S atoms in the disulfide bonds, possibly through a change of electron density distribution. To put it another way, the binding of the peptide to the (100) facet is realized by the interaction of a Cd atom with the disulfide bonds through electron sharing. This theoretical calculation result was substantiated by the SDS-PAGE and silver staining experiments. We chose the TGF-β1 protein, a small molecule in the form of dimeric ligands connected by a pair of disulfide bonds, to verify that breakage of the disulfide bonds is not needed for binding of the protein to CdSe-s materials. As expected, no monomer around 12.5 kDa was observed, in contrast to a pronounced band observed for DTT, which was used as a positive control (Figure S4). This corroborates the AIMD simulation result that protein molecules can be adsorbed onto the CdSe surface without breaking the disulfide bonds. Since different protein molecules have different structural flexibilities (as collectively determined by their molecular weight, hydrophobicity, charge distribution, etc.), their binding configurations (and accordingly binding energy) to a given surface would vary. Thus, while binding to Cd−S(e) surfaces is dominated by the interaction between Cd atoms and disulfide bonds, it is reasoned that both the abundance and distribution of the disulfide bonds would affect the binding configuration, leading to preferential binding of specific proteins. The fact that a few proteins with relatively high Cys% were not abundant in the corona of the Cd-containing nanoparticles (Table S1) was consistent with this argument.

3.4. Disrupting Structural Stability of Proteins May Be an Important Risk Factor Associated with Cd-Bearing Nanoparticles

Binding of proteins to the surfaces of Cd-containing nanoparticles can result in significant conformational changes of the proteins, the extent of which was facet-dependent. The CD spectra of BSA show that incubating with both CdSe-s-A and CdSe-s-B resulted in significant changes of the far-UV region (190−250 nm) of BSA, and a larger effect was observed on CdSe-s-A than on CdSe-s-B (Figure 5a); that is, the secondary

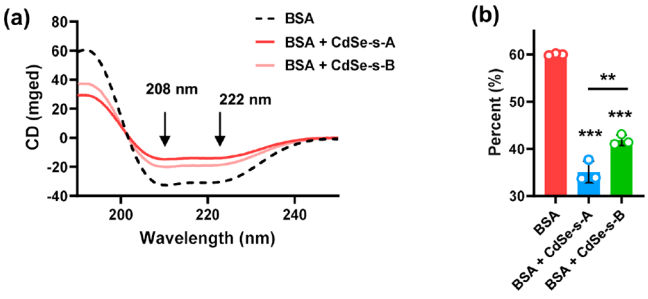

Figure 5. Effects of CdSe nanospheres on the structure of model proteins. (a,b) Circular dichroism (CD) spectra of BSA after exposure to CdSe nanospheres (a) and the relative changes of the α helix structures of BSA (b) upon adsorption. Data are presented as mean ± SD. Statistical significance between groups: (**) <0.01 and (***) <0.001; two-sided *t*-test.

structures of BSA were disrupted more significantly by CdSe-s-A. Specifically, when incubating with CdSe-s-A, the α-helix content of BSA decreased from 60.0% to 41.8%, but only to 35.1% when incubated with CdSe-s-B (Figure 5b). Disruption of protein structure compromises the physiological functions of proteins (e.g., reduced the enzyme activity)[36−38] and thus induces detrimental health effects (e.g., chronic pancreatitis, cystic fibrosis, and intestinal malabsorption).[39,40] This is particularly pertinent to some of the thiol-rich proteins (e.g., transferrin, complementary H and serum albumin), which have important biological functions (e.g., receptor-mediated endocytosis, immune activation, and maintaining osmotic pressure).[26] Understandably, this disrupting effect by Cd-containing nanoparticles on protein functions likely will be more significant for high-cysteine-content proteins and will be facet-dependent.

4. CONCLUSIONS

It is well recognized that the speciation of heavy metal contaminants dictates their environmental fate and effects. Mounting evidence indicates that nanoparticles, generated from both natural and anthropogenic sources, are important species of heavy metals and exhibit properties different from both their bulk-sized counterparts and dissolved forms. A unique characteristic of this species is that nanoparticles quickly acquire a protein corona upon biouptake, and this process largely determines their *in vivo* distribution, trans-

https://doi.org/10.1021/envhealth.4c00031
Environ. Health 2024, 2, 623−630

formation, and cytotoxicity.[26,41,42] This study underlines the critical role of the complex interactions between Cd-bearing nanoparticles and cysteine-rich proteins in determining the compositions of protein corona and, consequently, the biological effects of the nanoparticles.

The observed preferential binding of proteins, even between nanoparticles of essentially the same chemical compositions, size, shape, and electrokinetic properties, further emphasizes the critical role of the surface atomic configuration as regulated by the exposed facets in protein corona formation. Note that facet evolution is an important process of mineral formation and is largely dependent on environmental conditions. Additionally, facet engineering is commonly exploited in material design to maximize the performances. Thus, Cd-bearing nanoparticles in the environment likely will have varied facet compositions, leading to diverse protein corona compositions upon biouptake. Moreover, the simultaneous interactions of multiple binding groups of proteins with Cd-bearing nanoparticles are highly dynamic, dictated by the primary, secondary, and tertiary structures of a protein. Apparently, such complex interactions should not be over-simplified based on the interaction between a single binding group of protein (e.g., thiol group) and a Cd atom. The fact that facets and the abundance/distribution of binding groups of proteins collectively determine the binding configuration of proteins can be extended beyond Cd-containing nanoparticles, as any nanoparticle−protein combinations that allow strong complexation between multiple sites will likely exhibit similar effects.

It is widely accepted that the formation of a protein corona confers nanoparticles a biological identity that is markedly different from their pristine, uncoated counterparts. Clearly, this identity is regulated collectively by the surface atomic arrangement of the nanoparticles, as well as the specific biological media of concern. This should be taken into account when assessing the risks of soft metals in their nanoparticulate forms. The findings of this study also have important implications for the environmental and medical applications of nanomaterials. For example, facet engineering may be exploited to enable preferential or even selective binding of biomolecules such as peptides, proteins (e.g., antibodies), nucleic acids (e.g., aptamers), and lipids, for enhanced biocompatibility, cell recognition, and intracellular delivery.

■ ASSOCIATED CONTENT

Supporting Information

The Supporting Information is available free of charge at https://pubs.acs.org/doi/10.1021/envhealth.4c00031.

Details of materials and methods, additional results of hydrodynamic diameters and ζ potentials of Cd-based nanoparticles, information on proteins identified in the hard corona, kinetics of BSA adsorption on CdSe nanospheres, and the interaction between BSA and different facets (PDF)

■ AUTHOR INFORMATION

Corresponding Authors

Tong Zhang − *College of Environmental Science and Engineering, Ministry of Education Key Laboratory of Pollution Processes and Environmental Criteria, Tianjin Key Laboratory of Environmental Remediation and Pollution Control, Nankai University, Tianjin 300350, People's Republic of China;* orcid.org/0000-0002-8151-3697; Email: zhangtong@nankai.edu.cn

Chuanjia Jiang − *College of Environmental Science and Engineering, Ministry of Education Key Laboratory of Pollution Processes and Environmental Criteria, Tianjin Key Laboratory of Environmental Remediation and Pollution Control, Nankai University, Tianjin 300350, People's Republic of China;* orcid.org/0000-0003-2637-5508; Email: jiangcj@nankai.edu.cn

Authors

Yu Qi − *State Key Laboratory of Environmental Chemistry and Ecotoxicology, Research Center for Eco-Environmental Sciences, Chinese Academy of Sciences, Beijing 100085, People's Republic of China; University of Chinese Academy of Sciences, Beijing 100049, People's Republic of China; College of Environmental Science and Engineering, Ministry of Education Key Laboratory of Pollution Processes and Environmental Criteria, Tianjin Key Laboratory of Environmental Remediation and Pollution Control, Nankai University, Tianjin 300350, People's Republic of China;* orcid.org/0000-0002-4862-5347

Wenyu Guan − *College of Environmental Science and Engineering, Ministry of Education Key Laboratory of Pollution Processes and Environmental Criteria, Tianjin Key Laboratory of Environmental Remediation and Pollution Control, Nankai University, Tianjin 300350, People's Republic of China*

Wei Chen − *College of Environmental Science and Engineering, Ministry of Education Key Laboratory of Pollution Processes and Environmental Criteria, Tianjin Key Laboratory of Environmental Remediation and Pollution Control, Nankai University, Tianjin 300350, People's Republic of China;* orcid.org/0000-0003-2106-4284

Complete contact information is available at: https://pubs.acs.org/10.1021/envhealth.4c00031

Notes

The authors declare no competing financial interest.

■ ACKNOWLEDGMENTS

This research was supported by the National Natural Science Foundation of China (22125603, 22276211, and 22193051), and Tianjin Municipal Science and Technology Commission (21JCJQJC00060).

■ REFERENCES

(1) *Resource Conservation and Recovery Act*, U.S. Environmental Protection Agency.

(2) Hochella, M. F., Jr; Mogk, D. W.; Ranville, J.; Allen, I. C.; Luther, G. W.; Marr, L. C.; McGrail, B. P.; Murayama, M.; Qafoku, N. P.; Rosso, K. M.; Sahai, N.; Schroeder, P. A.; Vikesland, P.; Westerhoff, P.; Yang, Y. Natural, incidental, and engineered nanomaterials and their impacts on the Earth system. *Science* **2019**, *363*, eaau8299.

(3) Contreras, E. Q.; Cho, M.; Zhu, H.; Puppala, H. L.; Escalera, G.; Zhong, W.; Colvin, V. L. Toxicity of quantum dots and cadmium salt to Caenorhabditis elegans after multigenerational exposure. *Environ. Sci. Technol.* **2013**, *47*, 1148−1154.

(4) Tian, L. J.; Min, Y.; Li, W. W.; Chen, J. J.; Zhou, N. Q.; Zhu, T. T.; Li, D. B.; Ma, J. Y.; An, P. F.; Zheng, L. R.; Huang, H.; Liu, Y. Z.; Yu, H. Q. Substrate metabolism-driven assembly of high-quality CdS(x)Se(1- x) quantum dots in Escherichia coli: molecular mechanisms and bioimaging application. *ACS Nano* **2019**, *13*, 5841−5851.

(5) Gao, L.; Li, R.; Liang, Z.; Hou, L.; Chen, J. Seasonal variations of cadmium (Cd) speciation and mobility in sediments from the Xizhi River basin, South China, based on passive sampling techniques and a thermodynamic chemical equilibrium model. *Water Res.* **2021**, *207*, 117751−117762.
(6) Huang, M.; Liu, C.; Cui, P.; Wu, T.; Feng, X.; Huang, H.; Zhou, J.; Wang, Y. Facet-dependent photoinduced transformation of cadmium sulfide (CdS) nanoparticles. *Environ. Sci. Technol.* **2021**, *55*, 13132−13141.
(7) Gupta, G. S.; Kumar, A.; Senapati, V. A.; Pandey, A. K.; Shanker, R.; Dhawan, A. Laboratory scale microbial food chain to study bioaccumulation, biomagnification, and ecotoxicity of cadmium telluride quantum dots. *Environ. Sci. Technol.* **2017**, *51* (3), 1695−1706.
(8) Liu, W.; Weng, C.; Zheng, J.; Peng, X.; Zhang, J.; Lin, Z. Emerging investigator series: treatment and recycling of heavy metals from nanosludge. *Environ. Sci: Nano* **2019**, *6*, 1657−1673.
(9) Liu, H.; Gao, H.; Long, M.; Fu, H.; Alvarez, P. J. J.; Li, Q.; Zheng, S.; Qu, X.; Zhu, D. Sunlight promotes fast release of hazardous cadmium from widely-used commercial cadmium pigment. *Environ. Sci. Technol.* **2017**, *51*, 6877−6886.
(10) Li, C.; Chen, G.; Zhang, Y.; Wu, F.; Wang, Q. Advanced fluorescence imaging technology in the near-infrared-II window for biomedical applications. *J. Am. Chem. Soc.* **2020**, *142*, 14789−14804.
(11) Janković, N. Z.; Plata, D. L. Engineered nanomaterials in the context of global element cycles. *Environ. Sci: Nano* **2019**, *6*, 2697−2711.
(12) Allocca, M.; Mattera, L.; Bauduin, A.; Miedziak, B.; Moros, M.; De Trizio, L.; Tino, A.; Reiss, P.; Ambrosone, A.; Tortiglione, C. An integrated multilevel analysis profiling biosafety and toxicity induced by indium- and cadmium-based quantum dots in vivo. *Environ. Sci. Technol.* **2019**, *53*, 3938−3947.
(13) Oh, E.; Liu, R.; Nel, A.; Gemill, K. B.; Bilal, M.; Cohen, Y.; Medintz, I. L. Meta-analysis of cellular toxicity for cadmium-containing quantum dots. *Nat. Nanotechnol* **2016**, *11*, 479−486.
(14) Bi, X.; Feng, X.; Yang, Y.; Qiu, G.; Li, G.; Li, F.; Liu, T.; Fu, Z.; Jin, Z. Environmental contamination of heavy metals from zinc smelting areas in Hezhang County, western Guizhou, China. *Environ. Int.* **2006**, *32*, 883−890.
(15) Qi, Y.; Zhang, T.; Jing, C.; Liu, S.; Zhang, C.; Alvarez, P. J. J.; Chen, W. Nanocrystal facet modulation to enhance transferrin binding and cellular delivery. *Nat. Commun.* **2020**, *11*, 1262−1272.
(16) Du, T.; Shi, G.; Liu, F.; Zhang, T.; Chen, W. Sulfidation of Ag and ZnO nanomaterials significantly affects protein corona composition: implications for human exposure to environmentally aged nanomaterials. *Environ. Sci. Technol.* **2019**, *53*, 14296−14307.
(17) Wang, L.; Li, J.; Pan, J.; Jiang, X.; Ji, Y.; Li, Y.; Qu, Y.; Zhao, Y.; Wu, X.; Chen, C. Revealing the Binding Structure of the Protein Corona on Gold Nanorods Using Synchrotron Radiation-Based Techniques: Understanding the Reduced Damage in Cell Membranes. *J. Am. Chem. Soc.* **2013**, *135*, 17359−17368.
(18) Tan, Y.; Zhu, X.; Wu, D.; Song, E.; Song, Y. Compromised autophagic effect of polystyrene nanoplastics mediated by protein corona was recovered after lysosomal degradation of corona. *Environ. Sci. Technol.* **2020**, *54*, 11485−11493.
(19) Liu, X.; Yan, C.; Chen, K. L. Adsorption of human serum albumin on graphene oxide: implications for protein corona formation and conformation. *Environ. Sci. Technol.* **2019**, *53*, 8631−8639.
(20) Baimanov, D.; Wang, J.; Zhang, J.; Liu, K.; Cong, Y.; Shi, X.; Zhang, X.; Li, Y.; Li, X.; Qiao, R.; Zhao, Y.; Zhou, Y.; Wang, L.; Chen, C. In situ analysis of nanoparticle soft corona and dynamic evolution. *Nat. Commun.* **2022**, *13*, 5389−5403.
(21) Koffie, R. M.; Farrar, C. T.; Saidi, L. J.; William, C. M.; Hyman, B. T.; Spires-Jones, T. L. Nanoparticles enhance brain delivery of blood-brain barrier-impermeable probes for in vivo optical and magnetic resonance imaging. *Proc. Natl. Acad. Sci. U. S. A.* **2011**, *108*, 18837−18842.
(22) Salvati, A.; Pitek, A. S.; Monopoli, M. P.; Prapainop, K.; Bombelli, F. B.; Hristov, D. R.; Kelly, P. M.; Åberg, C.; Mahon, E.; Dawson, K. A. Transferrin-functionalized nanoparticles lose their targeting capabilities when a biomolecule corona adsorbs on the surface. *Nat. Nanotech* **2013**, *8*, 137−143.
(23) Herda, L. M.; Hristov, D. R.; Lo Giudice, M. C.; Polo, E.; Dawson, K. A. Mapping of Molecular Structure of the Nanoscale Surface in Bionanoparticles. *J. Am. Chem. Soc.* **2017**, *139*, 111−114.
(24) Lin, S.; Mortimer, M.; Chen, R.; Kakinen, A.; Riviere, J. E.; Davis, T. P.; Ding, F.; Ke, P. C. NanoEHS beyond Toxicity - Focusing on Biocorona. *Environ. Sci. Nano* **2017**, *4*, 1433−1454.
(25) Ke, P. C.; Lin, S.; Parak, W. J.; Davis, T. P.; Caruso, F. A Decade of the protein corona. *ACS Nano* **2017**, *11*, 11773−11776.
(26) Ren, J.; Andrikopoulos, N.; Velonia, K.; Tang, H.; Cai, R.; Ding, F.; Ke, P. C.; Chen, C. Chemical and biophysical signatures of the protein corona in nanomedicine. *J. Am. Chem. Soc.* **2022**, *144*, 9184−9205.
(27) Wang, Z.; Zhao, Q.; Cui, M.; Pang, S.; Wang, J.; Liu, Y.; Xie, L. Probing temperature- and pH-dependent binding between quantum dots and bovine serum albumin by fluorescence correlation spectroscopy. *Nanomater* **2017**, *7*, 93−106.
(28) He, Y.; Yin, P.; Gong, H.; Peng, J.; Liu, S.; Fan, X.; Yan, S. Characterization of the interaction between mercaptoethylamine capped CdTe quantum dots with human serum albumin and its analytical application. *Sens. Actuators, B* **2011**, *157*, 8−13.
(29) Liu, L.; Sun, M.; Zhang, H.; Yu, Q.; Li, M.; Qi, Y.; Zhang, C.; Gao, G.; Yuan, Y.; Zhai, H.; Chen, W.; Alvarez, P. J. Facet energy and reactivity versus cytotoxicity: the surprising behavior of CdS nanorods. *Nano Lett.* **2016**, *16*, 688−694.
(30) Majorek, K. A.; Porebski, P. J.; Dayal, A.; Zimmerman, M. D.; Jablonska, K.; Stewart, A. J.; Chruszcz, M.; Minor, W. Structural and immunologic characterization of bovine, horse, and rabbit serum albumins. *Mol. Immunol* **2012**, *52*, 174−182.
(31) Jain, A.; Ong, S. P.; Hautier, G.; Chen, W.; Richards, W. D.; Dacek, S.; Cholia, S.; Gunter, D.; Skinner, D.; Ceder, G.; Persson, K. A. Commentary: The materials project: a materials genome approach to accelerating materials innovation. *APL Mater.* **2013**, *1*, 11002−11013.
(32) Kresse, G.; Hafner, J. Ab initio molecular dynamics for liquid metals. *Phys. Rev. B* **1993**, *47*, 558−561.
(33) Ceperley, D. M.; Alder, B. J. Ground state of the electron gas by a stochastic method. *Phys. Rev. Lett.* **1980**, *45*, 566−569.
(34) Perdew, J. P.; Zunger, A. Self-interaction correction to density-functional approximations for many-electron systems. *Phys. Rev. B* **1981**, *23*, 5048−5079.
(35) Blöchl, P. E. Projector augmented-wave method. *Phys. Rev. B* **1994**, *50*, 17953−17979.
(36) Lynch, I.; Dawson, K. A. Protein-nanoparticle interactions. *Nano Today* **2008**, *3*, 40−47.
(37) Zeinabad, H. A.; Kachooei, E.; Saboury, A. A.; Kostova, I.; Attar, F.; Vaezzadeh, M.; Falahati, M. Thermodynamic and conformational changes of protein toward interaction with nanoparticles: a spectroscopic overview. *RSC Adv.* **2016**, *6*, 105903−105919.
(38) Wu, Z.; Zhang, B.; Yan, B. Regulation of enzyme activity through interactions with nanoparticles. *Int. J. Mol. Sci.* **2009**, *10*, 4198−4209.
(39) Zhou, J.; Sahin-Toth, M. Chymotrypsin C mutations in chronic pancreatitis. *J. Gastroenterol Hepatol* **2011**, *26*, 1238−1246.
(40) Littlewood, J. M.; Wolfe, S. P.; Conway, S. P. Diagnosis and treatment of intestinal malabsorption in cystic fibrosis. *Pediatr Pulmonol* **2006**, *41*, 35−49.
(41) Huang, R.; Carney, R. P.; Ikuma, K.; Stellacci, F.; Lau, B. L. T. Effects of surface compositional and structural heterogeneity on nanoparticle protein interactions: different protein configurations. *ACS Nano* **2014**, *8*, 5402−5412.
(42) Rabbani, G.; Ahn, S. N. Structure, enzymatic activities, glycation and therapeutic potential of human serum albumin: A natural cargo. *Int. J. Biol. Macromol.* **2019**, *123*, 979−990.

https://doi.org/10.1021/envhealth.4c00031
Environ. Health 2024, 2, 623−630